



## Short communication

## Novel zeolite-supported rhodium catalysts for ethanol steam reforming

Fabiana C. Campos-Skrobot<sup>a,1</sup>, Roberta C.P. Rizzo-Domingues<sup>b</sup>, Nádia R.C. Fernandes-Machado<sup>b</sup>, Mauricio P. Cantão<sup>a,\*</sup><sup>a</sup> LACTEC, Instituto de Tecnologia para o Desenvolvimento, C.P. 19067, 81531-980 Curitiba, PR, Brazil<sup>b</sup> UEM, Universidade Estadual de Maringá, Departamento de Engenharia Química, Av. Colombo, 5790 Bloco D-90, 87020-900 Maringá, PR, Brazil

## ARTICLE INFO

## Article history:

Received 8 April 2008

Received in revised form 7 May 2008

Accepted 8 May 2008

Available online 3 July 2008

## Keywords:

Ethanol

Steam reforming

Zeolite

Catalyst

Hydrogen

## ABSTRACT

Renewable bioethanol is an interesting hydrogen source for fuel cells through steam reforming, but its C–C bond promotes parallel reactions, mainly coke and by-products formation. In this way, good ethanol reforming catalysts are still needed, which explains current research and development efforts around the world. Most catalysts proposed for ethanol reforming are based on oxide-supported noble metals with surface area below  $100 \text{ m}^2 \text{ g}^{-1}$  and reaction temperatures above  $500^\circ\text{C}$ . Novel Rh and Rh–K catalysts supported on NaY zeolite with surface area above  $440 \text{ m}^2 \text{ g}^{-1}$  are presented in this work. Reaction temperature was fixed at  $300^\circ\text{C}$  and  $\text{H}_2\text{O}/\text{EtOH}$  molar ratio and reagent flow were varied. Ethanol conversion varied from 50 to 99%, with average increase of 50% due to K promoter, and hydrogen production yield achieved 68%.

© 2008 Elsevier B.V. All rights reserved.

## 1. Introduction

Biomass-based fuels have the potential to replace fossil fuels and mitigate greenhouse gas emissions and global warming. Sugar cane ethanol (EtOH) is the most promising biofuel, due to its economical feasibility and production of 8–10 times the energy consumed during the manufacturing, considering the whole chain of ethanol production and use [1]. Ethanol is largely used in Brazil, sharing 13% of vehicle fuels market.

Fuel cells and hydrogen are very attractive technologies for vehicle power and electricity generation. Well-to-wheel analysis shows the efficiency improvement: current internal combustion gasoline vehicles have efficiency around 15%, whereas FC vehicles based on gasoline reforming can achieve 24–31% [2]. Stationary phosphoric acid fuel cells (PAFC) electric efficiency can achieve 33%, compared to less than 25% for microturbines [3]. Simulation of electric generators composed of 1 kW polymer electrolyte fuel cells (PEMFC) and ethanol reformer has predicted an electric efficiency of 35% [4], while real small gasoline electric generators achieves 15%. It can be concluded that systems based on ethanol and fuel cells have the potential to combine efficient energy conversion technology with a renewable energy source.

Ethanol can be converted to hydrogen by means of steam or autothermal reforming and partial oxidation, using different catalysts and supports. Oxide-supported noble and non-noble metals have been tested, main catalysts being: Rh [5–13], Pd [7,8,14,15], Pt [7,8,15–17], Ru [8,18], Ir [19], Au [20], Ni [7,19,21–32], Co [6,15,19,24,26,31,33,34] and Cu, supported on  $\text{ZrO}_2$  [24] and  $\text{Nb}_2\text{O}_5$  [35,36]. Industrial dehydrogenation catalysts were also tested for steam reforming, with ethanol conversion below 40% [37].

Alumina-supported Rh was found to be one of the most active noble metal, showing higher activity and hydrogen selectivity in comparison to Pd, Pt, Ni and Ru [7,8]. Besides selectivity and conversion, surface area is also a very important parameter for catalytic reforming. Reported surface areas range around tens of  $\text{m}^2 \text{ g}^{-1}$ , but it is possible to achieve values above  $100 \text{ m}^2 \text{ g}^{-1}$  [14,16,22,30] or even  $200 \text{ m}^2 \text{ g}^{-1}$  [32] using oxide supports.

Alkali metals can be added to oxide-supported metal catalysts, aiming different effects on catalysis performance. K [27,28] and Li [28] promoters can improve sintering properties of Ni/MgO but have no influence on coke formation; otherwise, Li and Na have a negative effect on Ni dispersion in the same oxide [28]. Addition of Na to Co/ZnO catalysts has improved hydrogen production and catalyst stability, via inhibition of carbon deposition [34].  $\text{K}_2\text{O}$  and MgO have been added to Cu/ $\text{Nb}_2\text{O}_5$  and Cu–Ni/ $\text{Nb}_2\text{O}_5$ , improving conversion due to decreasing of niobium oxide acidity [36].

In this work Rh/NaY and Rh–K/NaY catalysts were prepared and used for ethanol steam reforming. NaY zeolite support has the prime function of increasing the surface area, aiming higher reforming reaction efficiency. Potassium was added to Rh/NaY

\* Corresponding author. Tel.: +55 41 3361 6200; fax: +55 41 3361 6007.

E-mail address: [cantao@lactec.org.br](mailto:cantao@lactec.org.br) (M.P. Cantão).<sup>1</sup> Present address: Federação das Indústrias do Paraná (FIEP), Av. Comendador Franco 1341, 80215-090 Curitiba, PR, Brazil.

catalyst in order to improve reforming performance, as it was verified by our group for Cu/Nb<sub>2</sub>O<sub>5</sub> [36]. Further experiments will confirm if this effect is related to decreasing of support acidity.

At our knowledge, this is the first test of zeolite-supported catalyst for ethanol reforming, although ZSM-5 zeolite had been previously used for CO<sub>2</sub> methane reforming [38].

## 2. Experimental

### 2.1. Catalysts preparation and characterization

NaY zeolite was prepared from aluminosilicate gel by mixing solutions of colloidal silica (46 g), sodium hydroxide (62 g), sodium aluminate (32 g) and distilled water (800 ml). The formed gel was transferred to a polyethylene bottle with threaded stopper, resting for 48 h at 95 °C to allow the crystallization. After cooled to room temperature, the solid product was filtrated, washed and dried at 100 °C during 24 h. Rh (5 wt%) and K (2 wt%) were added by impregnation of aqueous solution, then dried at 100 °C for 8 h and calcined at 500 °C during 4 h. Resulting catalyst powders were pressed in small tablets, ground and sieved to obtain pellets with diameter between 0.4 and 0.8 mm.

BET surface area was measured by nitrogen adsorption in a New Quantachrome b1200 instrument. For scanning electron microscopy (SEM) and energy dispersive X-ray spectrometry (EDS) a Hitachi S-4100 microscope was used. Atomic absorption spectroscopy (AAS) was performed on a PerkinElmer A Analyst 100 instrument. Crystalline phases were characterized by X-ray diffraction (XRD) in a Philips X'Pert model and temperature-programmed reduction (TPR) analyses were performed in a quartz reactor under 10%-H<sub>2</sub>/air flow from 25 to 950 °C at 15 °C min<sup>-1</sup> heating rate.

### 2.2. Catalytic testing

Ethanol steam reforming tests were carried out at 300 °C under atmospheric pressure in a cylindrical fixed-bed reactor containing 7.0 g of catalyst. This amount was fixed in order to replicate conditions closer to real operation. Catalyst sample was placed in reactor central part and silica gel with same mesh size was placed in the reactor ends. Experiments were conducted under reagent flow rates of 2.04 g min<sup>-1</sup> and 2.77 g min<sup>-1</sup> and under H<sub>2</sub>O/EtOH molar ratios of 3:1, 5:1 and 10:1. Catalytic reactions have been performed under the same conditions for both catalysts and were followed hourly during 3 h. The catalysts were previously activated at 300 °C under H<sub>2</sub> + N<sub>2</sub> stream during 4 h.

## 3. Results and discussion

### 3.1. Catalysts characterization

X-ray diffractograms and SEM micrographs of NaY and Rh/NaY samples are shown in Figs. 1 and 2, respectively. Zeolite samples have been adequately grown, with morphology in accordance with the literature [39]. Rh/NaY diffractogram (Fig. 1B) and micrograph (Fig. 2B) show morphology similar to that of the initial NaY zeolite. Diffractogram and SEM micrographs for Rh–K/NaY sample were the same as for Rh/NaY sample, indicating that K impregnation had no effect on catalyst morphology.

Atomic absorption analyses of Rh and Rh–K/NaY samples have confirmed metal catalyst and promoter content. AAS also showed that the Si/Al ratio is ca. 2.2 for the three samples, which was confirmed by SEM/EDS. The N<sub>2</sub> adsorption isotherms for zeolitic samples are of Type I, characteristic of microporous solids [39]. Surface areas for NaY, Rh/NaY and Rh–K/NaY, determined from the

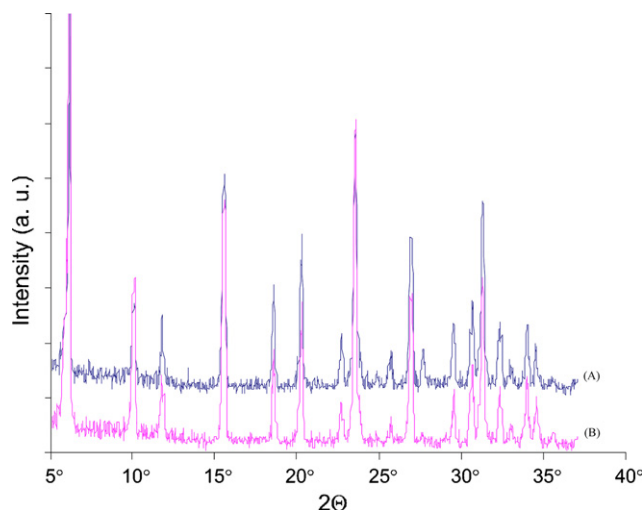


Fig. 1. X-ray diffractograms of NaY support (A) and Rh/NaY catalyst (B).

adsorption isotherm, are 647, 472 and 440 m<sup>2</sup> g<sup>-1</sup>, respectively. The decrease can be attributed to metallic particles blocking open pores and pathways to the surface.

Fig. 3 shows TPR scans for Rh/NaY and Rh–K/NaY. Reduction takes place between 70 and 200 °C, and the single peak indicates that Rh ions exist in one oxidation state. TPR scan for Rh–K/NaY

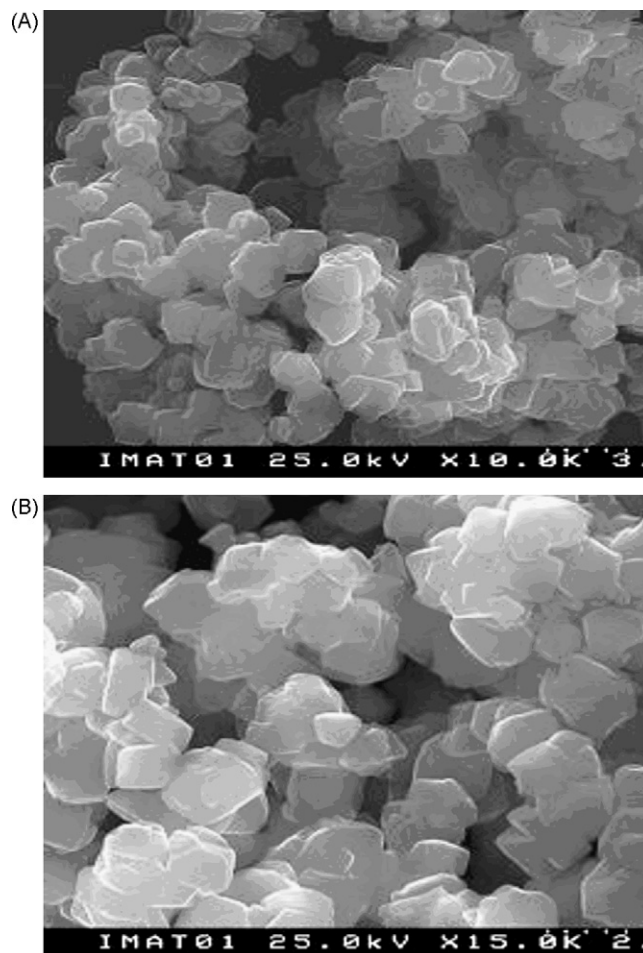


Fig. 2. SEM micrograph of (A) NaY support and (B) Rh/NaY catalyst.

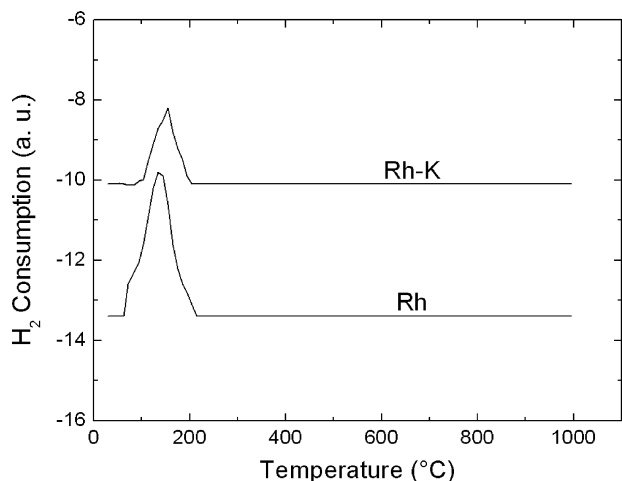


Fig. 3. TPR for Rh/NaY and Rh-K/NaY samples.

does not show reduction of K species, which remains as K<sub>2</sub>O after the activation. The only species in zeolite structure are Rh<sup>0</sup> and K<sub>2</sub>O.

### 3.2. Steam reforming catalytic reactions

Ethanol conversion and hydrogen yield are defined by the following equations:

$$\text{conversion} = \frac{\text{mol}(\text{consumed EtOH})}{\text{mol}(\text{EtOH entering reactor})} \times 100 \quad (1)$$

$$\text{H}_2 \text{ yield} = \frac{\text{mol}(\text{EtOH converted to H}_2)}{\text{mol}(\text{consumed EtOH})} \times 100 \quad (2)$$

No observed variation of conversion and yield was observed during the catalytic tests. However, stability behaviour is beyond scope of this work and will be addressed in further experiments. Figs. 4 and 5 show the effect of K promoter and of H<sub>2</sub>O/EtOH ratio on the total conversion. Conversion increases with H<sub>2</sub>O/EtOH ratio for both catalysts and reagent flows, but the effect is more pronounced with the presence of K species, which also turns the catalyst less sensitive on reagent flow.

Hydrogen yield also increases with H<sub>2</sub>O/EtOH ratio for both catalytic systems, as it can be seen in Fig. 6, but Fig. 7 shows that the effect is less evident for the higher reagent flow. For reagent flow

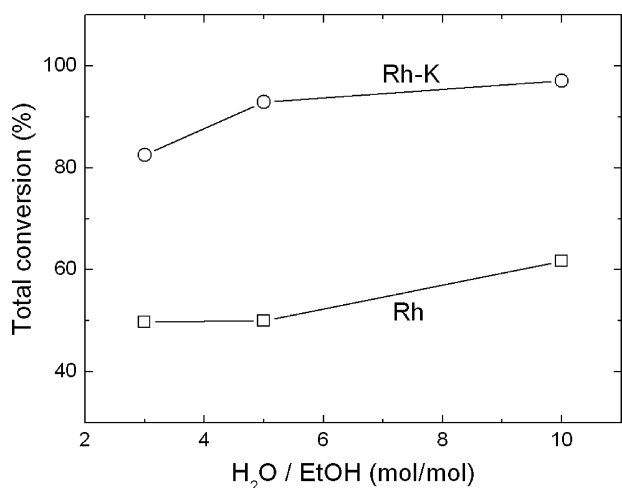


Fig. 4. Total conversion for Rh/NaY (□) and Rh-K/NaY (○), measured under 2.04 g min<sup>-1</sup> reagent flow.

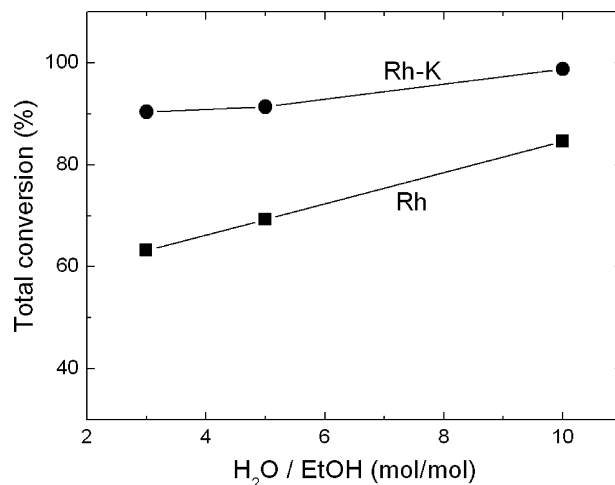


Fig. 5. Total conversion for Rh/NaY (■) and Rh-K/NaY (●), measured under 2.77 g min<sup>-1</sup> reagent flow.

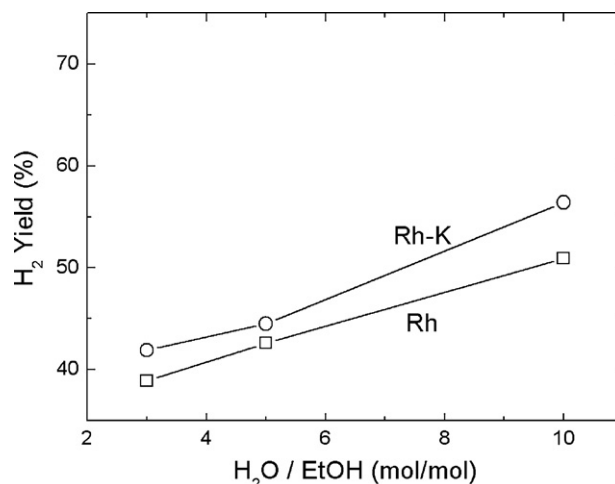


Fig. 6. Hydrogen yield for Rh/NaY (□) and Rh-K/NaY (○), measured under 2.04 g min<sup>-1</sup> reagent flow.

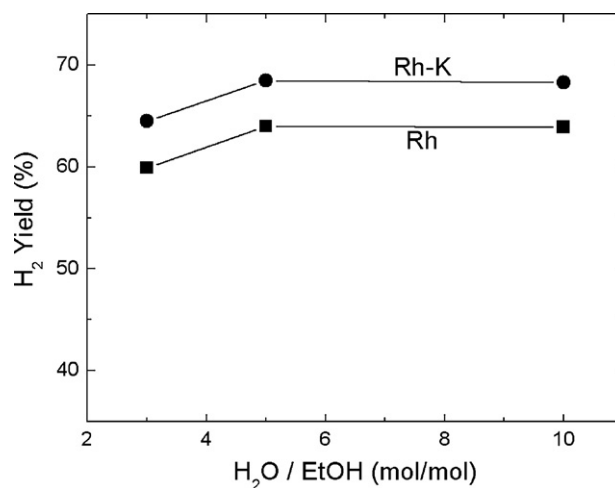


Fig. 7. Hydrogen yield for Rh/NaY (■) and Rh-K/NaY (●), measured under 2.77 g min<sup>-1</sup> reagent flow.

equal to  $2.77 \text{ g min}^{-1}$ , an increase by three times of  $\text{H}_2\text{O}/\text{EtOH}$  ratio results in less than 10% of conversion and hydrogen yield increase.

Results show that NaY-supported Rh catalysts are able to perform ethanol reforming and that higher water/ethanol ratios favour total conversion and hydrogen yield. Comparison with supports already studied [5–10,12] shows that total conversion is similar to some oxide-supported Rh catalysts, but most of oxides were tested at temperatures from 450 to  $850^\circ\text{C}$  [5–10].

Catalysts containing K present higher values of total conversion, as observed by Frusteri et al. [27], and a small increase was observed for hydrogen production. Frusteri et al. [28] have also observed that the addition of K promotes catalyst stability and prevents coke formation, effect not yet observed for Rh–K/NaY catalyst.

During reforming tests it was detected the presence of CO and  $\text{CH}_4$  by-products, but no content quantification was done. CO and  $\text{CH}_4$  production is not surprising, as most of ethanol reforming experiments report their production [5–34].

It is important to point out that Rh content was not optimized in the present study. Due to greater surface area of NaY zeolite it is reasonable to think that 5% Rh resulted in lower atomic surface density in comparison to oxide-supported catalysts. Together with stability, composition of zeolite-supported Rh and Rh–K needs to be studied in more detail.

#### 4. Conclusion

In this work novel zeolite-supported Rh catalysts were studied for ethanol steam reforming. It is shown that Rh/NaY is able to reform ethanol to hydrogen and that addition of K to the catalyst favours ethanol conversion, increasing it from 62 to 97%. Rh–K/NaY is also more effective for hydrogen formation. Best conversion values were achieved for higher  $\text{H}_2\text{O}/\text{EtOH}$  ratio and higher reagent flow, the latter being less effective for Rh–K/NaY catalyst. It was verified that reagent flow has greater influence on hydrogen yield than K addition. It is concluded that NaY zeolite-supported Rh can be considered promising catalysts for ethanol steam reforming, when compared with other existing studies.

#### Acknowledgements

F.C.C.-S. would like to thank the National Science and Technology Development Council (Conselho Nacional de Desenvolvimento Científico e Tecnológico, CNPq) for granting under contract no. 38.0276/2005-4. This work was funded by Parana State Energy Company (Companhia Paranaense de Energia, COPEL Geração), and for its support the authors are very grateful. M.P.C. would like to thank Eng. Mario Cesar do Nascimento (COPEL Geração) for his helpful contribution to this work.

#### References

[1] I.C. Macedo, M.R.L.V. Leal, J.E.A.R. da Silva, Assessment of Greenhouse Gas Emissions in the Production and Use of Fuel Ethanol in Brazil, Secretariat of the Environment, Government of the State of São Paulo, SP, Brazil, 2004.

[2] EG&G Technical Services, Inc., Fuel Cell Handbook, 7th ed., US Department of Energy, Morgantown, WV, 2004, p. 8–9.

[3] R.H. Camparin, L.A.C. Meleiro, R.M.M. Jorge, M.P. Cantão, P.R. Impinnisi, Quim. Nova 30 (2007) 1523–1528.

[4] J.A. Francesconi, M.C. Mussati, R.O. Mato, P.A. Aguirre, J. Power Sources 167 (2007) 151–161.

[5] S. Freni, J. Power Sources 94 (2001) 14–19.

[6] S. Cavallaro, N. Mondello, S. Freni, J. Power Sources 102 (2001) 198–204.

[7] J.P. Breen, R. Burch, H.M. Coleman, Appl. Catal. B: Environ. 39 (2002) 65–74.

[8] D.K. Liguras, D.I. Kondarides, X.E. Verykios, Appl. Catal. B: Environ. 43 (2003) 345–354.

[9] E.C. Wanat, K. Venkataraman, L.D. Schmidt, Appl. Catal. A: Gen. 276 (2004) 155–162.

[10] E. Vesselli, G. Comelli, R. Rosei, S. Freni, F. Frusteri, S. Cavallaro, Appl. Catal. A: Gen. 281 (2005) 139–147.

[11] W.-I. Hsiao, Y.-S. Lin, Y.-C. Chen, C.-S. Lee, Chem. Phys. Lett. 441 (2007) 294–299.

[12] C. Diagne, H. Idriss, K. Pearson, M.A. Gómez-García, A. Kiennemann, C.R. Chim. 7 (2004) 617–622.

[13] G.A. Deluga, J.R. Salge, L.D. Schmidt, X.E. Verykios, Science 303 (2004) 993–997.

[14] M.A. Goula, S.K. Kontou, P.E. Tsiakaras, Appl. Catal. B: Environ. 49 (2004) 135–144.

[15] L.V. Mattos, F.B. Noronha, J. Power Sources 152 (2005) 50–59.

[16] L.V. Mattos, F.B. Noronha, J. Power Sources 145 (2005) 10–15.

[17] L.V. Mattos, F.B. Noronha, J. Catal. 233 (2005) 453–463.

[18] D.K. Liguras, K. Goundani, X.E. Verykios, Int. J. Hydrogen Energy 29 (2004) 419–427.

[19] B. Zhang, X. Tang, Y. Li, Y. Xu, W. Shen, Int. J. Hydrogen Energy 32 (2007) 2367–2373.

[20] P.-Y. Sheng, G.A. Bowmaker, H. Idriss, Appl. Catal. A: Gen. 261 (2004) 171–181.

[21] J. Comas, F. Mariño, M. Laborde, N. Amadeo, Chem. Eng. J. 98 (2004) 61–68.

[22] S. Song, A.J. Akande, R.O. Iden, N. Mahinpey, Eng. Appl. Artif. Intel. 20 (2007) 261–271.

[23] F. Frusteri, S. Freni, V. Chiodo, S. Donato, G. Bonura, S. Cavallaro, Int. J. Hydrogen Energy 31 (2006) 2193–2199.

[24] M. Benito, J.L. Sanz, R. Isabel, R. Padilla, R. Arjona, L. Daza, J. Power Sources 151 (2005) 11–17.

[25] S. Freni, S. Cavallaro, N. Mondello, L. Spadaro, F. Frusteri, J. Power Sources 108 (2002) 53–57.

[26] S. Freni, S. Cavallaro, N. Mondello, L. Spadaro, F. Frusteri, Catal. Commun. 4 (2003) 259–268.

[27] F. Frusteri, S. Freni, V. Chiodo, L. Spadaro, G. Bonura, S. Cavallaro, J. Power Sources 132 (2004) 139–144.

[28] F. Frusteri, S. Freni, V. Chiodo, L. Spadaro, O. Di Blasi, G. Bonura, S. Cavallaro, Appl. Catal. A: Gen. 270 (2004) 1–7.

[29] J. Sun, X. Qiu, F. Wu, W. Zhu, W. Wang, S. Hao, Int. J. Hydrogen Energy 29 (2004) 1075–1081.

[30] D.K. Liguras, K. Goundani, X.E. Verykios, J. Power Sources 130 (2004) 30–37.

[31] J.A. Torres, J. Llorca, A. Casanovas, M. Domínguez, J. Salvadó, D. Montané, J. Power Sources 169 (2007) 158–166.

[32] M.C. Sánchez-Sánchez, R.M. Navarro, J.L.G. Fierro, Int. J. Hydrogen Energy 32 (2007) 1462–1471.

[33] A. Kaddouri, C. Mazzocchia, Catal. Commun. 5 (2004) 339–345.

[34] J. Llorca, N. Homs, J. Sales, J.-L.G. Fierro, J. Catal. 222 (2004) 470–480.

[35] N.R.C.F. Machado, M. Schmal, M.P. Cantão, R.C.P. Rizzo, L. Valgas, V. Calsavara, F. Takahashi, A.A. Almeida, F.R. Melo, M.A. Zschornack, A.N. Bessani, R.M.O. Rodrigues, Proceedings of the Hydrogen and Fuel Cells Conference and Trade Show, Vancouver, 2003.

[36] R.C.P.R. Domingues, N.R.C.F. Machado, M.P. Cantão, Acta Sci. Technol. 29 (2007) 1–7 (in Portuguese).

[37] L. Dolgykh, I. Stolyarchuk, I. Deynega, P. Strizhak, Int. J. Hydrogen Energy 31 (2006) 1607–1610.

[38] L. Wang, K. Murata, M. Inaba, Catal. Commun. 4 (2003) 147–151.

[39] D.W. Breck, Zeolite Molecular Sieves: Structure, Chemistry and Use, Krieger Publishing Company, New York, 1984.